

High-accuracy acoustic detection of nonclassical component of material nonlinearity

Sylvain Haupert,^{a)} Guillaume Renaud, Jacques Rivière, and Maryline Talmant
Laboratoire d'Imagerie Paramétrique, UPMC Univ Paris 06, CNRS, UMR 7623, Paris, France

Paul A. Johnson
Geophysics Group, Los Alamos National Laboratory, Los Alamos, New Mexico 87545

Pascal Laugier
Laboratoire d'Imagerie Paramétrique, UPMC Univ Paris 06, CNRS, UMR 7623, Paris, France

(Received 30 December 2010; revised 7 July 2011; accepted 24 August 2011)

The aim is to assess the nonclassical component of material nonlinearity in several classes of materials with weak, intermediate, and high nonlinear properties. In this contribution, an optimized nonlinear resonant ultrasound spectroscopy (NRUS) measuring and data processing protocol applied to small samples is described. The protocol is used to overcome the effects of environmental condition changes that take place during an experiment, and that may mask the intrinsic nonlinearity. External temperature fluctuation is identified as a primary source of measurement contamination. For instance, a variation of 0.1 °C produced a frequency variation of 0.01%, which is similar to the expected nonlinear frequency shift for weakly nonlinear materials. In order to overcome environmental effects, the reference frequency measurements are repeated before each excitation level and then used to compute nonlinear parameters. Using this approach, relative resonant frequency shifts of 10^{-5} can be measured, which is below the limit of 10^{-4} often considered as the limit of NRUS sensitivity under common experimental conditions. Due to enhanced sensitivity resulting from the correction procedure applied in this work, nonclassical nonlinearity in materials that before have been assumed to only be classically nonlinear in past work (steel, brass, and aluminum) is reported. © 2011 Acoustical Society of America. [DOI: 10.1121/1.3641405]

PACS number(s): 43.25.Zx, 43.25.Ba, 43.25.Ed, 43.25.Gf [OAS]

Pages: 2654–2661

I. INTRODUCTION

The evolution of material nonlinearity is of great interest for nondestructive evaluation and structural health monitoring. In homogeneous elastic materials, only classical lattice nonlinearity arising from weak anharmonicity of the interatomic potential is typical (Landau and Lifshitz, 1986). In contrast, microinhomogeneous solids (such as rocks, or damage materials) exhibit a significant increase of elastic material nonlinearity arising from strongly enhanced strains at the soft defects (i.e., grain boundary, cracks) (Ostrovsky and Johnson, 2001; Guyer and Johnson, 2009). Such mesoscopic nonlinearity arising from the presence of soft defects in an elastic matrix can be considered as nonclassical as opposed to the purely classical lattice nonlinearity. Nonclassical nonlinearity differs from classical lattice nonlinearity not only quantitatively, but also with qualitative distinctive features such as hysteretic character and simultaneous amplitude-dependent variations in elasticity and dissipation (Guyer *et al.*, 1995; Guyer and Johnson, 2009). Several recent literature reports evidenced that, in microinhomogeneous and damaged solids, other mechanisms which are linear and nonhysteretic by nature, such as dissipation mechanisms (e.g., thermoelastic or viscous losses) arising at the very same soft structural defects also contribute to the overall amplitude-dependent dissipation, and thus to the non-

classical mesoscopic material nonlinearity (Zaitsev and Sas, 2000; Gusev and Tournat, 2005; Fillinger *et al.*, 2006; Zaitsev and Matveev, 2006).

A number of nonlinear acoustic techniques based on harmonic generation (Breazeale and Thompson, 1963; Morris *et al.*, 1979; Cantrell and Yost, 2001), frequency mixing (Van den Abeele *et al.*, 2000b; Donskoy *et al.*, 2001; Courtney *et al.*, 2008), acousto-elastic effect (Nagy, 1998; Renaud *et al.*, 2009), dynamic resonance characteristics (Van den Abeele *et al.*, 2000a; Nazarov *et al.*, 2009), cross-modulation technique (Zaitsev *et al.*, 2006), cascade modulation method (Zaitsev *et al.*, 2011), or cascade cross-modulation (Zaitsev *et al.*, 2008) have been developed to monitor damage and progressive damage in various materials such as concrete (Van den Abeele and De Visscher, 2000; Bentahar *et al.*, 2006; Payan *et al.*, 2007; Bruno *et al.*, 2009), metallic structures (Nazarov and Kolpakov, 2000; Straka *et al.*, 2008; Zagrai *et al.*, 2008), composites (Van den Abeele *et al.*, 2001; Meo *et al.*, 2008; Van Den Abeele *et al.*, 2009; Aymerich and Staszewski, 2010), and more recently in human cortical bone (Muller *et al.*, 2008) and trabecular bone (Renaud *et al.*, 2008; Moreschi *et al.*, 2011).

This work has been motivated by the importance of detecting microdamage accumulation in bone specimens using nondestructive methods (Muller *et al.*, 2005; Muller *et al.*, 2008). This requires high-accuracy measurements that are sensitive specifically to small defects (i.e., microdamage) concentration. To this purpose, nonlinear acoustical techniques such as harmonic generation or conventional

^{a)}Author to whom correspondence should be addressed. Electronic mail: sylvain.haupt@upmc.fr

modulation interactions, in which the contribution of a small amount of microdamage to the material nonlinearity can be masked by the classical nonlinearity, may not be an appropriate choice. In contrast, the intentional use of acoustical techniques that are highly sensitive to nonclassical nonlinear effects which can be considered as being the signature of the presence of damage must be favored. Among these are unconventional modulation techniques (Zaitsev *et al.*, 2006; Zaitsev *et al.*, 2008; Zaitsev *et al.*, 2009, 2011) and nonlinear resonant ultrasound spectroscopy (NRUS) (Johnson *et al.*, 1996; Van den Abeele *et al.*, 2000a) that allow one to reduce the masking role of the classical nonlinearity. NRUS, which allows the observation of simultaneous amplitude-dependent variations in elastic modulus and dissipation, has been shown to be extremely sensitive to intrinsic damage in several materials, including human bone (Muller *et al.*, 2005; Bentahar *et al.*, 2006; Payan *et al.*, 2007; Muller *et al.*, 2008; Zacharias *et al.*, 2009; Chen *et al.*, 2010; Rivière *et al.*, 2010). This is also a primary drawback since NRUS is also very sensitive to numerous other factors, including temperature, humidity, and bonding quality, which may affect the measured nonlinear response and may hinder recovery of the desired nonlinear properties of the material. Measurement errors and poor precision are among the key points to solve in order to broadly apply nonlinear methods to practical problems and increase their sensitivity of detection of subtle variations in microdamage.

In this study, we present an optimized NRUS method, to minimize measurement errors and maximize precision. Our goal is to assess the elastic and dissipative nonclassical nonlinear parameters as well as the variability in these parameters, using several classes of materials with weak, intermediate, and high nonlinear properties. The protocol outlined here can be modified for other nonlinear acoustics procedures as well. In Sec. II, we present the theoretical background for NRUS measurements of nonclassical nonlinearity, assuming that it arises purely from quadratic hysteretic mechanisms. The measurement protocol of simultaneous amplitude-dependent variations in the elasticity and dissipation with careful compensation of thermal effects is detailed in Sec. III, whereas results are presented in Sec. IV. Section V offers a discussion of the data observed in several classes of materials taking into account several mechanisms contributing to the observed nonclassical nonlinearity.

II. BACKGROUND

Hysteretic elastic behaviors [also called nonclassical, nonlinear mesoscopic (Guyer and Johnson, 2009) and nonlinear-nonequilibrium (Pasqualini *et al.*, 2007)] are usually interpreted at the mesoscopic scale as a consequence of the presence of intrinsic damage (disbonding, micro-cracks, dislocation-point defect interactions, glassy dynamics) and may include nonlinear internal friction (dislocations, grain boundary effects, recovery bonds) and structural properties (geometrically flat porosity and irregular geometry resulting in stress localization). In contrast, “classical” nonlinearity of the Landau type is due to atomic anharmonicity (Landau and Lifshitz, 1986). It is commonly observed that the hysteretic

regime is visible for strains above 10^{-7} – 10^{-6} in experiments conducted at ambient pressure in Earth and damaged solids (TenCate *et al.*, 2004). In a typical NRUS experiment, the sample is probed using a swept frequency wave at an eigenmode of the sample, applying progressively increasing drive amplitude level (Johnson and Sutin, 2005). Hysteretic (nonclassical) nonlinearity is manifest as a resonance frequency shift and damping for increasing voltage drive level which is proportional to the peak strain amplitude (Guyer *et al.*, 1995). One of the most widely used models is a phenomenological description based on the Preisach–Mayergoyz space (PM space) (Guyer *et al.*, 1995). The following represents the nonlinear stress–strain relationship:

$$\sigma(\varepsilon, \dot{\varepsilon}) = K_0 \left(\varepsilon - \beta \varepsilon^2 - \delta \varepsilon^3 + \frac{\alpha}{2} \left[2(\Delta\varepsilon)\varepsilon - \text{sign}(\dot{\varepsilon})((\Delta\varepsilon)^2 - \varepsilon^2) \right] \right), \quad (1)$$

where K_0 , σ , ε , $\dot{\varepsilon}$, and $\Delta\varepsilon$ are the linear modulus, the stress, the instantaneous strain, the time derivative of the instantaneous strain, and the maximum strain excursion over a wave cycle, respectively. The modulus K can be derived from this model by combining the classical nonlinear parameters β and δ from Landau theory with the hysteretic nonlinear parameter α .

When hysteretic nonlinearities exceed classical nonlinearities [generally for strains above approximately 10^{-6} (Johnson and Sutin, 2005)], two nonlinear parameters α_f and α_Q describing the frequency shift Δf and the change of energy loss as a function of strain, respectively, can be derived from Eq. (1):

$$\frac{f - f_0}{f_0} = \frac{\Delta f}{f_0} = \frac{\alpha_f}{2} \Delta\varepsilon, \quad (2)$$

$$\frac{1}{Q} - \frac{1}{Q_0} = \frac{\alpha_Q}{2} \Delta\varepsilon, \quad (3)$$

where f and Q are the resonance frequency and Q -factor (inversely proportional to the modal damping ratio) at increased strain level, f_0 and Q_0 their corresponding value at the lowest drive amplitude (often presumed to be elastically linear if the initial drive amplitude is low enough) (Johnson and Sutin, 2005). Both α_f and α_Q are related to the general nonlinear parameter α of Eq. (1) (Guyer *et al.*, 1995).

The Read ratio $\pi\alpha_Q/2\alpha_f$ between the complementary variation in the decrement ($\pi\Delta Q^{-1}$) and complementary relative variation in the elastic modulus ($\Delta K/K_0 \approx 2\Delta f/f_0$), introduced to characterize hysteretic nonlinearities (Read, 1940), is expected to be equal to 4/3 for purely quadratic hysteretic nonlinearity (Lebedev, 1999).

III. MATERIALS AND METHODS

A. Samples

Specimens from different classes of materials were tested: (1) polymers [poly(methyl methacrylate) (PMMA) and polyvinyl chloride (PVC)] known to exhibit no

hysteretic behavior but only small classical nonlinearities and commonly used as test standards (Johnson *et al.*, 2004); (2) geomaterials (chalk and travertine) exhibiting highly nonlinear hysteretic elasticity; (3) polycrystalline metals (stainless steel 304, brass, aluminum AU4G) generally considered to be linear or weakly nonlinear, and (4) dry bovine cortical bone. PMMA and PVC were tested to be certain that the electrical system and contact nonlinearities had no influence. For each material, three samples were tested for repeatability three times each with intermediate repositioning (except for PVC, chalk, and travertine, only two samples). All samples have the same parallelepiped shape with size 2 mm × 4 mm × 50 mm, except for chalk (6 mm × 6 mm × 65 mm) and travertine rock (4 mm × 8 mm × 50 mm). These dimensions were chosen as being optimal for the four-point bending mechanical fatigue tests that will be conducted in ongoing studies with cortical bone.

B. NRUS

Each sample was probed by a swept-sine encompassing the first three modes of the material (assumed to be pure compression modes under symmetric loading conditions). The frequency band around the resonance frequency is $f_0 \pm \Delta f$, where $\Delta f = 5\%$. The source consisted of a piezoceramic emitter bonded to the sample with cyanoacrylate glue. The sample was placed on a foam block to avoid contact nonlinearity. The input signal was a linear chirp centered on f_0 , the resonance frequency at the lowest drive amplitude. The frequency sweep duration, $t \gg Q/(\pi f_0)$, ranging from 100 ms to 1 s, was heuristically chosen as a compromise to prevent inducing temperature increase of the sample while at the same time reaching as to as possible a steady state at each frequency during the sweep. The voltage amplitude of the input signal was carefully adapted to each sample (1) to induce minimum strain peak amplitude larger than 10^{-6} consistent with a hysteretic regime and (2) a maximum strain level lower than 10^{-4} to prevent sample damage and piezoceramics debonding. A reference resonance curve was first obtained at the lowest strain level. The resonance frequency f_0 (also energy loss Q_0^{-1}) was determined and used as a reference frequency (reference energy loss). The peak resonance frequency f and energy loss Q^{-1} were then measured as a function of strain applying increasing voltage drive level. The experimental protocol was carefully designed to ensure that the excitation duration and voltage level do not generate slow dynamics for all materials. To this goal, we applied the method described by Johnson and Sutin (2005) with specific excitation duration of 1 s. A delay of 3 s between each drive level test was used to minimize memory and conditioning effects [slow dynamics (TenCate and Shankland, 1996)] and to allow the samples to recover to their initial state before each sequential excitation amplitude. The time interval was based on repeated tests to determine the duration of the material slow dynamics. The nonlinear parameters α_f and α_Q were extracted from a linear fit to the experimental data according to Eqs. (2) and (3). In this procedure, the sample is assumed to remain in the same state for all the excitation drive levels as it was at the lowest drive level (i.e., no tem-

perature change, no damage or slow dynamics conditioning occurring over the course of a single experiment) (Pasqualini *et al.*, 2007). The dynamic strain amplitude ε was calculated from the longitudinal particle displacement u measured by a laser vibrometer LSV 1 MHz (SIOS, Germany), the phase velocity c (determined by time of flight method), and the frequency f_0 :

$$\varepsilon = \frac{2\pi f_0}{c} u. \quad (4)$$

During the experiments, room temperature was controlled ($25^\circ\text{C} \pm 2^\circ\text{C}$). The sample was placed in a polystyrene box to minimize local temperature variations. The sample temperature was monitored by noncontact infrared thermometer with a resolution of 0.02°C .

C. Data processing

Since both the resonance frequency and attenuation are known to vary with temperature, samples require substantial care in terms of controlling the temperature. In order to avoid such error sources, frequently efforts are made to enclose the sample in a climate chamber. For example, Pasqualini *et al.* (2007) described stringent experimental conditions to achieve long-term frequency stability of $\pm 0.1\text{Hz}$ with a long-term thermal stability of 10 mK. Such conditions could not be reached with our experimental chamber. Our observations revealed that temperature fluctuations could be of the order of $\pm 0.5^\circ\text{C}$ over the course of a single experiment [Fig. 1(a)]. Hence, the determination of frequency and damping shifts as functions of strain is complicated by the fact that external conditions (e.g., temperature) lead to shifts in frequency and damping (e.g., via heating) which can be as large as that caused by intrinsic material nonlinearity (Fig. 2). To overcome this effect, we adopted an approach inspired by Pasqualini *et al.* (2007).

The initial reference resonance curve was obtained at the lowest strain level. The excitation level was increased and a new resonance curve was obtained. Then the resonance reference curve was repeated at the lowest drive level. This procedure was repeated at progressively increasing excitation drive levels, so that n reference resonance frequencies $f_{0,n}$ were collected. If the sample remains in the same state over the course of the experiment (e.g., no change of temperature), the repeated resonance curve at the lowest strain level should match the initial reference curve. If temperature changes, the repeated frequency curve peak resonance $f_{0,n}$ will change. An example is shown for a bone sample in Fig. 1, where temperature changes of -0.7°C and $+0.2^\circ\text{C}$ are observed during two repeated NRUS measurements. Variations in reference resonance frequency $f_{0,n}$ mirror those of temperature, indicating that temperature indeed is the main source of these variations. Temperature will also affect the peak resonance frequency at higher excitation drive level [Fig. 2(a)]. Note that if slow mechanics was essential at the considered excitation levels, its effect on low drive reference curve should be reproducible. This is not the case, as illustrated in Fig. 1. The reference curve is mainly correlated

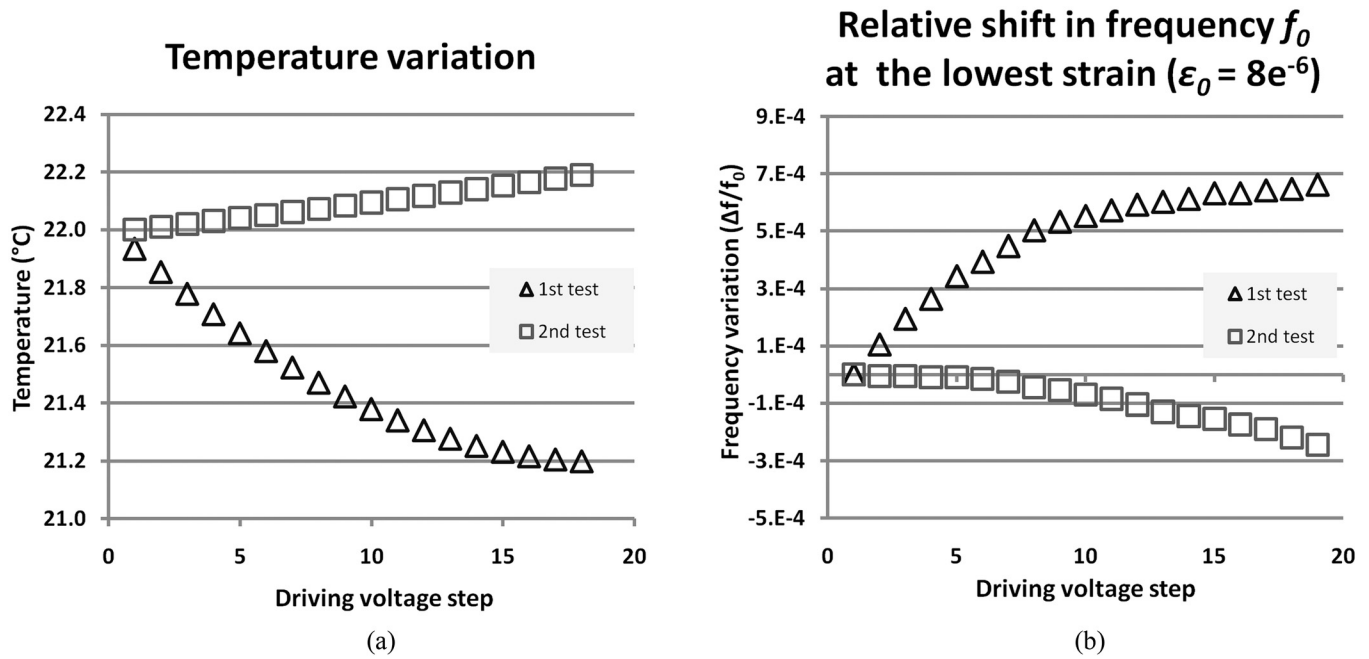


FIG. 1. Bone sample, first mode. (a) Temperature variations recorded at the sample surface during two different NRUS experiments. (b) Corresponding shift in $f_{0,n}$ (lowest excitation level).

with temperature variations that are due to the room temperature regulation.

Therefore, applying Eqs. (2) and (3) with the initial reference resonance peak frequency f_0 to derive α_f and α_Q , will lead to erroneous values. A correction can be applied by using $f_{0,n}$ instead of f_0 in Eqs. (2) and (3). Using this correction, at each excitation level, the shift in f and Q^{-1} is now relative to the environmentally modified $f_{0,n}$ and $Q_{0,n}^{-1}$. An example is illustrated in Fig. 2 for the bone specimen (same data as those in Fig. 1). While the uncorrected frequency shift [Fig. 2(a)] displays variations with strain mirroring tem-

perature changes, we found a repeatable linear relationship between corrected frequency shift and strain, as predicted by quadratic hysteresis elastic nonlinearity [Eq. (1)]. This suggests the efficiency of the procedure to correct undesirable material state variations and to capture intrinsic nonclassical nonlinear properties. Temperature was found to be less influential on energy loss (data not shown). The correction was applied to all the specimens. In the following, we detail results obtained for all the materials. The repeatability is assessed via the coefficient of variation $CV\% = SD/\mu$, where SD and μ are the standard deviation and mean value obtained

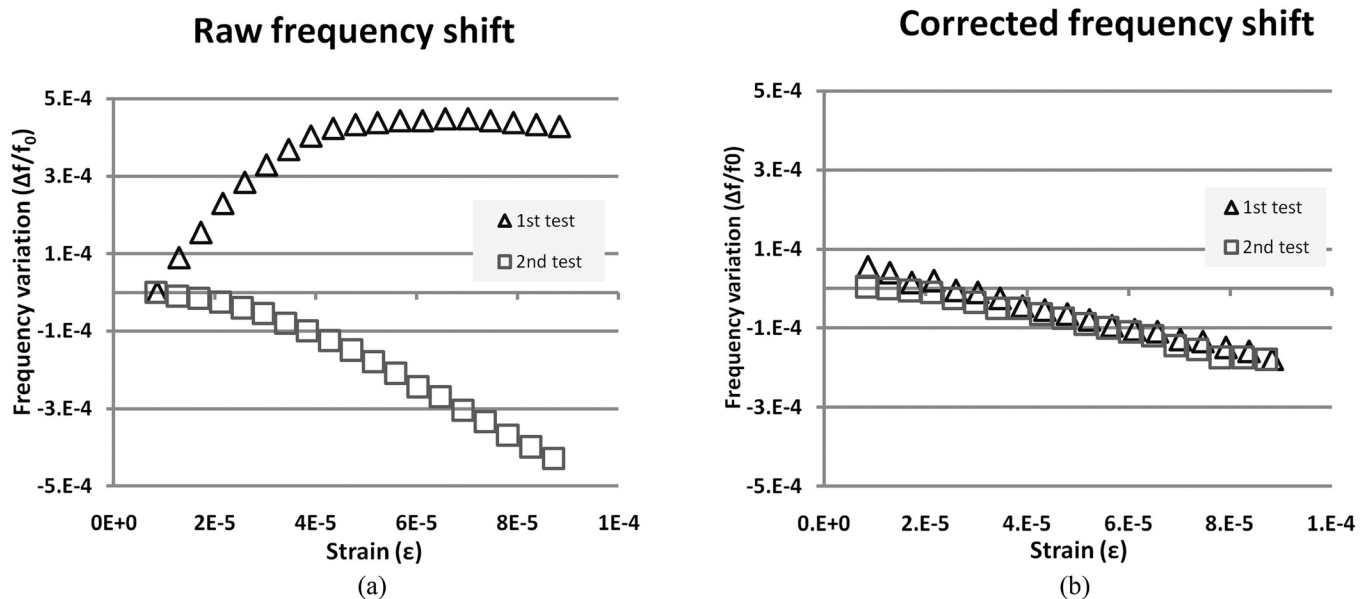


FIG. 2. Bone sample, first mode. (a) Frequency shift computed with Eq. (2) obtained during two different NRUS experiments. (b) Corrected frequency shift computed with Eq. (2) where f_0 is replaced by $f_{0,n}$. Temperature effects, if uncorrected, may result in frequency shifts (a) that overpass intrinsic nonlinear frequency shifts (b).

for three repeated measurements with intermediate repositioning.

IV. RESULTS

Figure 3 shows the corrected frequency and damping shifts for all materials tested (second compression mode). The absence of variation for polymers (PMMA and PVC) even for high strain levels up to 5×10^{-5} confirms that our experimental setup is linear. For all other materials (chalk, bone, stainless steel, aluminum, and brass), a quasi-linear dependence with strain was found for both the elastic and dissipative parts of the complex modulus.

Table I shows the coefficients of variation of uncorrected and corrected α_f and α_Q . The correction yielded significantly reduced CVs, especially in the case of bone, aluminum, and brass, the three materials with the weakest nonlinear properties. For these materials, and particularly for bone (uncorrected data, CV of 201.9%; corrected data, CV of 16.2%), the variation in uncorrected resonance frequency would mostly reflect the influence of temperature. Without correction, intrinsic weak nonlinear behavior could not be observed. In contrast, moderate or no change in CV was obtained after correction for the three materials with the highest nonlinear properties (stainless steel, pastel chalk, and travertine). Note that the reduction in CVs was more pronounced for α_f than for α_Q , indicating that the resonance frequency is more influenced by environmental factors than damping. In summary, our results illustrate that the correction procedure is useful to enhance the sensitivity of NRUS, especially for weakly nonlinear materials and is useful in retrieving weak nonlinear properties.

Mean values of α_f and α_Q for the first three compression modes are summarized in Tables II and III. Nonlinear properties are weak for bone, aluminum, and brass ($\alpha_f = -5.0.2$ to -29.9 and $\alpha_Q = 2.1-22.6$). These properties were found to be one order of magnitude higher for stainless steel 304

TABLE I. Mean coefficient of variation (CV) of nonlinear parameters (α_f , α_Q) before and after correction (no data for PMMA and PVC, which are linear).

	α_f variability (CV)		α_Q variability (CV)	
	Uncorrected (%)	Corrected (%)	Uncorrected (%)	Corrected (%)
Bovine bone	201.9	16.2	19.5	14.2
Aluminum	30.8	6.2	5.8	4.2
Brass	13.6	6.9	7.0	6.5
Stainless steel	5.4	4.9	4.8	3.6
Pastel chalk	5.1	3.1	7.0	7.3
Travertine	7.1	7.0	13.4	21.7

($\alpha_f > -113$ and $\alpha_Q > 90.6$) and chalk ($\alpha_f = -39.3$ to -256.1 and $\alpha_Q = 13.5-80.4$). Travertine (a calcium carbonate rich precipitate rock) is the most nonlinear material ($\alpha_f = -1238$ to -1401 and $\alpha_Q = 192-228$). With α_f ranging from -5.0 to -6.9 and α_Q ranging from -2.1 to -3.6 , dry cortical bovine bone manifests the smallest nonlinear properties. Note that values of α_f and α_Q could not be measured for the first mode of brass and stainless steel, due to overlapping resonant peaks.

While the Read ratio $\pi\alpha_Q/2\alpha_f$ was found close to 4/3 for metallic samples (aluminum: 1.03 for mode 1, 1.31 and 1.36 for modes 2 and 3, respectively; brass: 1.09 and 1.19 for modes 1 and 2, respectively; steel: 1.28 and 1.25 for modes 2 and 3, respectively), strong variations were observed for other materials (bone: 0.61–1.13; pastel chalk: 0.46–0.80; travertine: 0.26–0.80).

V. DISCUSSION

High-accuracy measurements of the complementary variations in the elasticity and dissipation with careful compensation of thermal effects are made for the first time. Simultaneous amplitude-dependent variations in the elasticity

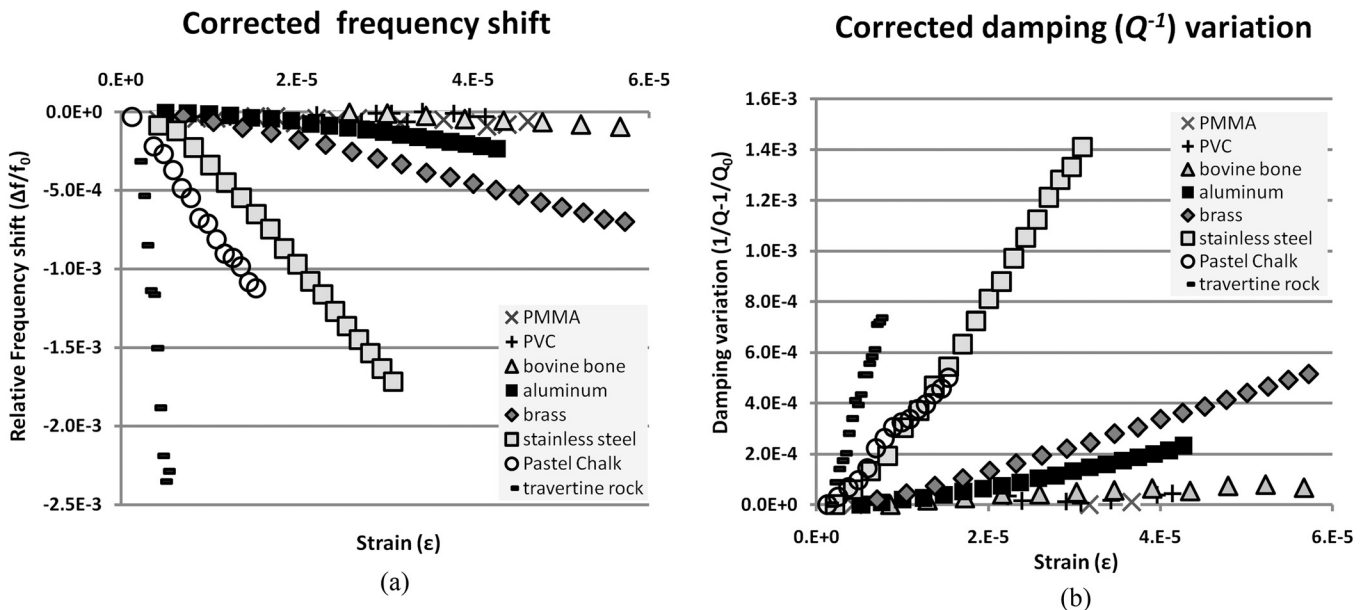


FIG. 3. Frequency (a) and damping (b) (second compression mode) dependence on strain level for all materials tested (one sample of each).

TABLE II. Mean hysteretic reactive parameter (α_f).

	$\alpha_{f \text{ mode } 1}$	$\alpha_{f \text{ mode } 2}$	$\alpha_{f \text{ mode } 3}$
Bovine bone	-5.0 ± 2.5	-5.1 ± 0.3	-6.9 ± 0.6
Aluminum	-12.2 ± 2.2	-16.3 ± 0.4	-19.5 ± 1.5
Brass	—	-27.3 ± 3.2	-29.9 ± 1.2
Stainless steel	—	-120.0 ± 9.6	-113.9 ± 11.6
Pastel chalk	-39.3 ± 1.4	-157 ± 6.8	-256.1 ± 6.2
Travertine	-1377.8 ± 71.7	-1401.2 ± 141.6	1238.6 ± 72.2

(α_f) and dissipation (α_Q) are specific signatures of hysteretic nonlinearity of soft structural defects. However, our data need careful interpretation, because in the case of nonlinearity induced by the presence of soft defects, the situation may be more complex, since very similar simultaneous amplitude-dependent variations in the elasticity and dissipation can also arise from nonhysteretic mechanisms such as thermoelastic or viscous losses (Zaitsev and Sas, 2000; Fillingier *et al.*, 2006; Zaitsev and Matveev, 2006).

The amplitude dependence of dissipation and modulus are well fitted by a linear law for all the measured materials, as expected from quadratic hysteretic nonlinearity. Deviations from a linear dependence have been observed by others due to a combination of classical cubic-in-strain nonlinearity of the lattice with quadratic hysteresis (Pasqualini *et al.*, 2007), to a nonquadratic hysteresis such as shown by Nazarov in lead (Nazarov, 1999) or zinc (Nazarov and Kolpakov, 2000). In our case, given the relatively narrow range of variation of the amplitude excitation (over one order of magnitude only), our data could be approximated by a linear fit as well as with a power law with good accuracy. Thus, we think that our experimental data do not allow concluding on the linear (i.e., purely quadratic hysteretic) or nonlinear (i.e., not purely hysteretic or nonquadratic hysteretic) amplitude dependence of elasticity and dissipation. To reach the conclusion that a power law or a polynomial function yields a better prediction, a greater strain range would be required.

Mean values of α_f and α_Q are consistent for the three measured modes in bone, aluminum, brass, steel, travertine (Table III), meaning that the nonlinearity is quasi-frequency independent. Small discrepancies observed between the different modes (bone, aluminum, brass, steel, travertine) may be due to measurement errors. They can also be attributed to differences in the contributions of the different modes to the nonlinearity because of the spatial inhomogeneity in the distribution of soft defects in the samples or of the modal strain amplitude that has been found to explain a significant amount of the variation of α_f and α_Q between modes (Van

TABLE III. Mean hysteretic dissipative parameter (α_Q).

	$\alpha_{Q \text{ mode } 1}$	$\alpha_{Q \text{ mode } 2}$	$\alpha_{Q \text{ mode } 3}$
Bovine bone	3.6 ± 2.5	2.1 ± 0.3	2.7 ± 0.6
Aluminum	8 ± 2.2	13.6 ± 0.4	16.9 ± 1.5
Brass	—	18.9 ± 3.2	22.6 ± 1.2
Stainless steel	—	98.2 ± 9.6	90.6 ± 11.6
Pastel chalk	13.5 ± 0.5	80.4 ± 11.1	74.5 ± 2.6
Travertine	192.9 ± 49.8	228.3 ± 46.5	204.3 ± 38.6

Den Abeele, 2007). For pastel chalk, the nonlinear characteristics of mode 1 deviates substantially from those of modes 2 and 3 (Table III). In this case, the spatial distribution of nodes and anti-nodes is not sufficient to explain the observed increase of α_f and α_Q with resonant frequency. Actually, besides producing additional amplitude-dependent dissipation, the effective viscoelastic properties of the defects can lead to a very pronounced frequency-dependent variation of the material nonlinearity (Zaitsev *et al.*, 2001; Zaitsev *et al.*, 2002; Zaitsev and Matveev, 2006). These corrections are different for different materials, and in the case of pastel chalk, the strong discrepancy between the nonlinearity observed for different modes may arise from such a nonhysteretic mechanism competing with the genuine intrinsic hysteretic behavior. The separation of the respective contribution of the two mechanisms (the hysteretic one and the nonhysteretic one) to the material nonlinearity would require additional experiments.

If we compare the so-called Read ratio ($\pi\alpha_Q/2\alpha_f$) for different materials, the experimentally observed ratios differ over 5 times. Read ratios of polycrystalline metals (aluminum, brass, and stainless steel) are within 5–20% accuracy, close to 4/3 expected for the quasi-static quadratic hysteresis. This suggests that the nonhysteretic source of material nonlinearity mentioned earlier is not significant for the metallic samples measured in this work. For other materials (cortical bone, chalk, and travertine rock) the difference is much stronger: The Read ratio can be much lower than the theoretical value (e.g., for travertine rocks, the Read ratio is 0.25). This strong discrepancy in the apparent Read's parameter can be understood if we take into account that the finite relaxation time of the defects (their effective viscosity) produces corrections to the complementary variations in the elasticity and dissipation as mentioned earlier. Obviously, these corrections are different for different materials, so that the apparent Read ratio can vary strongly between different materials.

Our values for geomaterials are consistent with values reported previously in the literature (Johnson and Sutin, 2005). Some results on polycrystalline metals can be found in Nazarov *et al.* (1988); Nazarov (1991); Nazarov and Kolpakov (2000). Hysteretic elastic behavior for stainless steel, aluminum, and brass has rarely been observed [brass (Jon *et al.*, 1976); aluminum (Chambers and Smoluchowski, 1960); steel (Masumoto *et al.*, 1979)], whereas it is well known in polycrystalline metals such as zinc (Read, 1940; Lebedev *et al.*, 1993; Nazarov and Kolpakov, 2000), copper (Nowick, 1950), Cu-based alloys (Kustov *et al.*, 2006), and ternary carbide, Ti_3SiC_2 (Finkel *et al.*, 2009).

We note that the results may be affected by damage induced when cutting the samples as well as by thermal treatment (quenching, annealing) inherent to the metallic plate's production. While our experiments do not strictly allow eliminating extra damage induced by sample preparation, the higher nonlinearity observed in steel compared to other metallic samples may have its source in larger grain mobility due to the coexistence of two phases (perlite + ferrite α). Interestingly, complementary measurements achieved in the laboratory (data not shown) on a

stainless steel 304 specimen with different sample preparation (no cutting was performed, except to both ends), different shape (rod), larger dimensions (200 mm in length and 30 mm in diameter), and lower resonant frequency (6 kHz) yielded comparable results, which supports the assumption that the intrinsic quadratic hysteretic behavior of stainless steel 304 was indeed measured on the small specimen. This result is remarkable, and suggests that given sufficient noise reducing procedures, other metals and single crystals considered classically nonlinear of the Landau type should be tested as well. The paradigm of hysteretic nonlinearity may extend far beyond the materials currently considered as such.

VI. CONCLUSIONS

In this contribution, we presented a new data processing to analyze NRUS data obtained on small specimens, in which the frequency shift Δf is measured relative to a reference resonance peak curve $f_{0,n}$ (obtained at the lowest excitation level) which is repeated before each excitation drive level. Our results show that the correction procedure may be used as an alternative to stringent temperature control by increasing significantly NRUS precision and sensitivity. With our correction procedure, we measured relative resonant frequency shifts of 10^{-5} , well below 10^{-4} , often considered the limit to NRUS sensitivity under common experimental conditions. Enhanced sensitivity would permit measurement of weak manifestation of nonclassical nonlinear elasticity of soft structural defects in materials such as bone, and monitoring subtle changes in nonlinear properties induced by damage accumulation (e.g., occurring during a progressive damage test).

In our experiments, we identified external temperature fluctuations as the major source of resonance frequency variation. A variation of 0.1°C at the bone sample surface caused a frequency variation of 0.01% (Fig. 1), which is similar to the expected nonlinear frequency shift for weakly nonlinear materials. In the absence of correction, the data could not be interpreted to support the existence of nonclassical nonlinear behavior in bone (Fig. 2). Besides temperature, other factors may affect the elastic response of a material (and its resonance) and compete with material intrinsic nonlinearity. These include environmental factors (e.g., humidity, pressure), conditioning and long-time relaxation effects (TenCate *et al.*, 2004). The advantage of our correction procedure is that (1) it allows for differences in the starting values of f_0 whatever the origin of these differences and (2) that it automatically corrects for these differences, except if environmental factor variation is large and fast enough to change the nonlinearity itself during measurement (Van Den Abeele *et al.*, 2002) which should not be the case under ambient conditions. Applying the method, nonhysteretic viscous-like and/or thermoelastic mechanisms cannot be easily disentangled from genuine hysteretic mechanisms, as both hysteretic and nonhysteretic phenomena compete during NRUS measurements. In order to isolate the nonhysteretic contribution to elastic and dissipative nonlinear variation, one should consider working at frequencies not

affected by frequency-dependent attenuation (e.g., using quasi-static measurements) or at different modes over the larger possible frequency band.

Finally, we report nonlinear values for a number of materials. Thanks to the correction procedure applied in this work, we report nonclassical nonlinearity in materials (steel, brass, and aluminum) that were generally assumed to be only classically nonlinear in past work.

ACKNOWLEDGMENTS

The authors want to acknowledge the reviewers for their helpful and constructive comments. This research was supported by the Agence Nationale pour la Recherche (ANR), France (Grant No. BONUS_07BLAN0197). P.A.J. was supported in part by Institutional Support at Los Alamos National Laboratory and by the Office of Basic Energy Science of the US Department of Energy.

- Aymerich, F., and Staszewski, W. (2010). "Experimental study of impact-damage detection in composite laminates using a cross-modulation vibro-acoustic technique," *Struct. Health Monit.* **9**, 541.
- Bentahar, M., El Agra, H., El Guerjouma, R., Griffa, M., and Scalerandi, M. (2006). "Hysteretic elasticity in damaged concrete: Quantitative analysis of slow and fast dynamics," *Phys. Rev. B* **73**, 014116.
- Breazeale, M., and Thompson, D. (1963). "Finite amplitude ultrasonic waves in aluminum," *Appl. Phys. Lett.* **3**, 77.
- Bruno, C., Gliozzi, A., Scalerandi, M., and Antonaci, P. (2009). "Analysis of elastic nonlinearity using the scaling subtraction method," *Phys. Rev. B* **79**, 064108.
- Cantrell, J., and Yost, W. (2001). "Nonlinear ultrasonic characterization of fatigue microstructures," *Int. J. Fatigue* **23**, 487–490.
- Chambers, R., and Smoluchowski, R. (1960). "Time-dependent internal friction in aluminum and magnesium single crystals," *Phys. Rev.* **117**, 725–731.
- Chen, J., Jayapalan, A. R., Kim, J. Y., Kurtis, K. E., and Jacobs, L. J. (2010). "Rapid evaluation of alkali-silica reactivity of aggregates using a nonlinear resonance spectroscopy technique," *Cem. Concr. Res.* **40**, 914–923.
- Courtney, C., Drinkwater, B., Neild, S., and Wilcox, P. (2008). "Factors affecting the ultrasonic intermodulation crack detection technique using bispectral analysis," *NDT & E Int.* **41**, 223–234.
- Donskoy, D., Sutin, A., and Ekimov, A. (2001). "Nonlinear acoustic interaction on contact interfaces and its use for nondestructive testing," *NDT & E Int.* **34**, 231–238.
- Fillinger, L., Zaitsev, V. Y., Gusev, V., and Castagnede, B. (2006). "Nonlinear relaxational absorption/transparency for acoustic waves due to thermoelastic effect," *Acta Acust. Acust.* **92**, 24–34.
- Finkel, P., Zhou, A. G., Basu, S., Yeheskel, O., and Barsoum, M. W. (2009). "Direct observation of nonlinear acoustoelastic hysteresis in kinking nonlinear elastic solids," *Appl. Phys. Lett.* **94**, 241904.
- Gusev, V., and Tournat, V. (2005). "Amplitude- and frequency-dependent nonlinearities in the presence of thermally-induced transitions in the Preisach model of acoustic hysteresis," *Phys. Rev. B* **72**, 054104.
- Guyer, R., McCall, K., and Boitnott, G. (1995). "Hysteresis, discrete memory, and nonlinear wave propagation in rock: A new paradigm," *Phys. Rev. Lett.* **74**, 3491–3494.
- Guyer, R. A., and Johnson, P. A. (2009). *Nonlinear Mesoscopic Elasticity: The Complex Behaviour of Rocks, Soil, Concrete* (Wiley-VCH, Weinheim), pp. 1–410.
- Johnson, P., and Sutin, A. (2005). "Slow dynamics and anomalous nonlinear fast dynamics in diverse solids," *J. Acoust. Soc. Am.* **117**, 124–130.
- Johnson, P. A., Zinszner, B., Rasolofosaon, P., Cohen-Tenoudji, F., and Van Den Abeele, K. (2004). "Dynamic measurements of the nonlinear elastic parameter alpha in rock under varying conditions," *J. Geophys. Res. [Solid Earth]* **109**, B02202.
- Johnson, P. A., Zinszner, B., and Rasolofosaon, P. N. J. (1996). "Resonance and elastic nonlinear phenomena in rock," *J. Geophys. Res. [Solid Earth]* **101**, 11553–11564.

- Jon, M., Mason, W., and Beshers, D. (1976). "Internal friction during ultrasonic deformation of alpha brass," *J. Appl. Phys.* **47**, 2337–2349.
- Kustov, S., Golyandin, S., Ichino, A., and Gremaud, G. (2006). "A new design of automated piezoelectric composite oscillator technique," *Mater. Sci. Eng., A* **442**, 532–537.
- Landau, L., and Lifshitz, E. (1986). *Theory of Elasticity* (Pergamon, Oxford), pp. 1–187.
- Lebedev, A. B. (1999). "Amplitude-dependent elastic-modulus defect in the main dislocation-hysteresis models," *Phys. Solid State* **41**, 1105–1111.
- Lebedev, A. B., Burenkov, Y. A., and Golubenko, T. I. (1993). "Internal-friction and acoustoplastic effect in zinc single-crystals under deformation," *Fiz. Tverd. Tela (St. Petersburg)* **35**, 420–430.
- Masumoto, H., Sawaya, S., and Hinai, M. (1979). "On the damping capacity of Fe-Cr alloys," *Mater. Trans. JIM* **20**, 409–413.
- Meo, M., Polimeno, U., and Zumpano, G. (2008). "Detecting damage in composite material using nonlinear elastic wave spectroscopy methods," *Appl. Compos. Mater.* **15**, 115–126.
- Moreschi, H., Callé, S., Guerard, S., Mitton, D., Renaud, G., and Defontaine, M. (2011). "Monitoring trabecular bone microdamage using a dynamic acousto-elastic testing method," *Proc. Inst. Mech. Eng., Part H: J. Eng. Med.* **225**, 1–12.
- Morris, W. L., Buck, O., and Inman, R. V. (1979). "Acoustic harmonic-generation due to fatigue damage in high-strength aluminum," *J. Appl. Phys.* **50**, 6737–6741.
- Muller, M., Mitton, D., Talmant, M., Johnson, P., and Laugier, P. (2008). "Nonlinear ultrasound can detect accumulated damage in human bone," *J. Biomech.* **41**, 1062–1068.
- Muller, M., Sutin, A., Guyer, R., Talmant, M., Laugier, P., and Johnson, P. A. (2005). "Nonlinear resonant ultrasound spectroscopy (NRUS) applied to damage assessment in bone," *J. Acoust. Soc. Am.* **118**, 3946–3952.
- Nagy, P. B. (1998). "Fatigue damage assessment by nonlinear ultrasonic materials characterization," *Ultrasonics* **36**, 375–381.
- Nazarov, V. E. (1991). "Nonlinear acoustical effects in annealed copper," *Sov. Phys. Acoust.* **37**, 75–78.
- Nazarov, V. E. (1999). "Amplitude-dependent internal friction of lead," *Fiz. Met. Metalloved.* **88**, 82–90.
- Nazarov, V. E., and Kolpakov, A. B. (2000). "Experimental investigations of nonlinear acoustic phenomena in polycrystalline zinc," *J. Acoust. Soc. Am.* **107**, 1915–1921.
- Nazarov, V. E., Kolpakov, A. B., and Radostin, A. V. (2009). "Amplitude dependent internal friction and generation of harmonics in granite resonator," *Acoust. Phys.* **55**, 100–107.
- Nazarov, V. E., Ostrovsky, L. A., Soustova, I. A., and Sutin, A. M. (1988). "Nonlinear acoustics of micro-inhomogeneous media," *Phys. Earth Planet. Inter.* **50**, 65–73.
- Nowick, A. S. (1950). "Variation of amplitude-dependent internal friction in single crystals of copper with frequency and temperature," *Phys. Rev.* **80**, 249–257.
- Ostrovsky, L. A., and Johnson, P. A. (2001). "Dynamic nonlinear elasticity in geomaterials," *Riv. Nuovo Cimento* **24**, 1–46.
- Pasqualini, D., Heitmann, K., TenCate, J. A., Habib, S., Higdon, D., and Johnson, P. A. (2007). "Nonequilibrium and nonlinear dynamics in Berea and Fontainebleau sandstones: Low-strain regime," *J. Geophys. Res. [Solid Earth]* **112**, B01204.
- Payan, C., Garnier, V., Moysan, J., and Johnson, P. A. (2007). "Applying nonlinear resonant ultrasound spectroscopy to improving thermal damage assessment in concrete," *J. Acoust. Soc. Am.* **121**, EL125–EL130.
- Read, T. A. (1940). "The internal friction of single metal crystals," *Phys. Rev.* **58**, 371–380.
- Renaud, G., Callé, S., and Defontaine, M. (2009). "Remote dynamic acoustoelastic testing: Elastic and dissipative acoustic nonlinearities measured under hydrostatic tension and compression," *Appl. Phys. Lett.* **94**, 011905.
- Renaud, G., Calle, S., Remenieras, J. P., and Defontaine, M. (2008). "Exploration of trabecular bone nonlinear elasticity using time-of-flight modulation," *IEEE Trans. Ultrason. Ferroelectr. Freq. Control* **55**, 1497–1507.
- Rivière, J., Renaud, G., Hauptert, S., Talmant, M., Laugier, P., and Johnson, P. (2010). "Nonlinear acoustic resonances to probe a threaded interface," *J. Appl. Phys.* **107**, 4901.
- Straka, L., Yagodzinsky, Y., Landa, M., and Hänninen, H. (2008). "Detection of structural damage of aluminum alloy 6082 using elastic wave modulation spectroscopy," *NDT & E Int.* **41**, 554–563.
- TenCate, J. A., Pasqualini, D., Habib, S., Heitmann, K., Higdon, D., and Johnson, P. A. (2004). "Nonlinear and nonequilibrium dynamics in geomaterials," *Phys. Rev. Lett.* **93**, 065501.
- TenCate, J. A., and Shankland, T. J. (1996). "Slow dynamics in the nonlinear elastic response of Berea sandstone," *Geophys. Res. Lett.* **23**, 3019–3022.
- Van Den Abeele, K. (2007). "Multi-mode nonlinear resonance ultrasound spectroscopy for defect imaging: An analytical approach for the one-dimensional case," *J. Acoust. Soc. Am.* **122**, 73–90.
- Van Den Abeele, K., Carmeliet, J., Johnson, P., and Zinszner, B. (2002). "Influence of water saturation on the nonlinear elastic mesoscopic response in Earth materials and the implications to the mechanism of nonlinearity," *J. Geophys. Res.* **107**, 2121.
- Van den Abeele, K., and De Visscher, J. (2000). "Damage assessment in reinforced concrete using spectral and temporal nonlinear vibration techniques," *Cem. Concr. Res.* **30**, 1453–1464.
- Van Den Abeele, K., Le Bas, P., Van Damme, B., and Katkowski, T. (2009). "Quantification of material nonlinearity in relation to microdamage density using nonlinear reverberation spectroscopy: Experimental and theoretical study," *J. Acoust. Soc. Am.* **126**, 963–972.
- Van den Abeele, K., Van de Velde, K., and Carmeliet, J. (2001). "Inferring the degradation of pultruded composites from dynamic nonlinear resonance measurements," *Polym. Compos.* **22**, 555–567.
- Van den Abeele, K. E. A., Carmeliet, J., Ten Cate, J. A., and Johnson, P. A. (2000a). "Nonlinear elastic wave spectroscopy (NEWS) techniques to discern material damage, part II: Single-mode nonlinear resonance acoustic spectroscopy," *Res. Nondestruct. Eval.* **12**, 31–42.
- Van den Abeele, K. E. A., Johnson, P. A., and Sutin, A. (2000b). "Nonlinear elastic wave spectroscopy (NEWS) techniques to discern material damage, part I: Nonlinear wave modulation spectroscopy (NWMS)," *Res. Nondestruct. Eval.* **12**, 17–30.
- Zacharias, K., Balabanidou, E., Hatzokos, I., Rekanos, I. T., and Trochidis, A. (2009). "Microdamage evaluation in human trabecular bone based on nonlinear ultrasound vibro-modulation (NUVM)," *J. Biomech.* **42**, 581–586.
- Zagrai, A., Donskoy, D., Chudnovsky, A., and Golovin, E. (2008). "Micro- and macroscale damage detection using the nonlinear acoustic vibro-modulation technique," *Res. Nondestructive Eval.* **19**, 104–128.
- Zaitsev, V., Gusev, V., and Castagnede, B. (2002). "Luxemburg-Gorky effect retooled for elastic waves: A mechanism and experimental evidence," *Phys. Rev. Lett.* **89**, 105502.
- Zaitsev, V., Nazarov, V., Gusev, V., and Castagnede, B. (2006). "Novel nonlinear-modulation acoustic technique for crack detection," *NDT & E Int.* **39**, 184–194.
- Zaitsev, V. Y., and Matveev, L. (2006). "Microinhomogeneous medium, elastic nonlinearity, linear dissipation, amplitude dependent dissipation," *Russ. Geol. Geophys.* **47**, 694–709.
- Zaitsev, V. Y., Matveev, L., Matveev, A., and Arnold, W. (2008). "Cascade cross modulation due to the nonlinear interaction of elastic waves in samples with cracks," *Acoust. Phys.* **54**, 398–406.
- Zaitsev, V. Y., Matveev, L., and Matveyev, A. (2009). "On the ultimate sensitivity of nonlinear-modulation method of crack detection," *NDT & E Int.* **42**, 622–629.
- Zaitsev, V. Y., Matveev, L., and Matveyev, A. (2011). "Elastic-wave modulation approach to crack detection: Comparison of conventional modulation and higher-order interactions," *NDT & E Int.* **44**, 21–31.
- Zaitsev, V. Y., Nazarov, V., and Belyaeva, I. Y. (2001). "The equation of state of a microinhomogeneous medium and the frequency dependence of its elastic nonlinearity," *Acoust. Phys.* **47**, 178–183.
- Zaitsev, V. Y., and Sas, P. (2000). "Dissipation in microinhomogeneous solids: Inherent amplitude-dependent attenuation of a non-hysteretical and non-frictional type," *Acust. Acta Acust.* **86**, 429–445.